Proceedings of
The Second National Congress on Fluids Engineering
August 22-24, 2002, Muju, Korea

원자로 사고 또는 과도상태시 공기방출현상에 대한 연구

배윤영*, 김환열†, 송철화†, 김희동†,

Study of Air Clearing during Severe Transient of Nuclear Reactor Coolant System

Yoon Yeong Bae*, Hwan Yeol Kim†, Chul-Hwa Song†, Hee Dong Kim†

***Key words**: Sparger(증기분사기), Air bubble(공기방울), Oscillation(진동)*

Abstract

An experiment has been performed using a facility, which simulates the safety depressurization system (SDS) and in-containment refueling water storage tank (IRWST) of APR1400, an advanced PWR being developed in Korea, to investigate the dynamic load resulting from the blowdown of steam from a steam generator through a sparger. The influence of the key parameters, such as air mass, steam pressure, submergence, valve opening time, and pool temperature, on frequency and peak loads was investigated. The blowdown phenomenon was analyzed to find out the real cause of the initiation of bubble oscillation and discrepancy in frequencies between the experiment and calculation by conventional equation for bubble oscillation. The cause of significant damping was discussed and is presumed to be the highly tortuous flow path around bubble. The Rayleigh-Plesset equation, which is modified by introducing method of image, reasonably reproduces the bubble oscillation in a confined tank. Right after the completion of air discharge the steam discharge immediately follows and it condenses abruptly to provide low-pressure pocket. It may contribute to the negative maximum being greater than positive maximum. The subsequently discharging steam does not play as the driving force anymore.

1. INTRODUCTION

The design of APR1400**, an advanced PWR, introduces IRWST, into which steam or two-phase fluid from reactor coolant system discharges in case of severe system transient. The phenomena likely to occur in these systems, are expected to be similar to those occurred in BWR dry well and wet well, although the degree and time scale would not be the same. When the safety valve between reactor vessel and SDS opens due to accident or severe transient, high pressure steam discharges into SDS and compresses air in SDS piping, prior to discharge of water, which fills the submerged part of piping (Bae et al. 2000). Then the water, compressed air, and steam discharge successively. The accurate estimation of magnitude and frequency of the oscillation of the air bubble is the major concern of the plant designer for the design of containment structure. A sparger (or quencher) is introduced first in BWR to reduce dynamic load due to steam condensation and air bubble oscillation. Among the types of sparger used in BWRs an I-type sparger developed by ABB-Westinghouse for BWR in Sweden is adopted in APR1400.

The loads due to the safety/relief valve quencher(or sparger) for BWR Mark II and III containment are summarized in NUREG-0802 (T. M. Su, 1982). This report evaluated various cases and resulting loads, pressure and frequency, and recommended acceptance criteria. However the information contained in NUREG-0801 cannot be applied directly to our case, since the operating conditions as well as geometrical parameters are different. Furthermore there does not exist any accepted formula or scaling method to deduce useful information from the existing one. Therefore test of full-scale sprager is performed to find plant information specific to APR1400.

The oscillation of small bubbles in infinite medium due to sound wave and cavitation has been successfully analyzed by an equation derived by Rayleigh (1917), where the bubble size is extremely small, less than 0.01 mm, and the effect of damping - viscous, thermal, and radiation - and surface tension is significant. However, when the bubble size is large (0.01 mm or larger), the effect of viscosity and surface tension is negligible (Leighton, 1994). Our interest in this paper falls into this category.

In this paper the results of a full-scale experiment performed at KAERI Boiling and Condensation loop are briefly reviewed. The peak dynamic pressure and oscillation frequencies obtained from experiment will be compared with the analytic estimation. The applicability of Rayleigh-Plesset equation is discussed and in order to reflect the damping the modification method is suggested.

2. EXPERIMENT

The experimental facility is shown in Fig. 1. The facility

* Korea Atomic Energy Research Institute, Advanced ReactorDevelopment Div., corresponding author, yybae@kaeri.re.k

† Korea Atomic Energy Research Institute, Advanced ReactorDevelopment Div.

** Trade mark of KEPCO and KHNP

consists of pressurizer, discharge piping, vacuum breaker, quench tank (simulates IRWST), steam generator, water storage tank, air compressor, charging pump, and sparger. The conditions of the experiment are

- Pressurizer pressure: up to 157 bar
- Pool temperature: 40 - 95°C
- Steam mass flux: 1250 – 3350 kg/m^{2}s
- Water level from the tank bottom: 3.6 m

Since the diameter of piping is less than prototype, an air chamber is added in the piping to make the air mass the same as that of prototype, 1.5 kg. By pressurizing the air chamber up to proper condition the prescribed air mass is insured.

Fig. 2 shows typical pressure history in the piping during blowdown period. The pressure about 150 bar drops sharply to less than around 10 bar(g) at the sparger head. An orifice is installed in the piping so that most of the pressure drop occurs before sprager and the pressure at the sparger be as close to the prototype as possible. By close examination of the pressure variations shown in Fig. 2 it is known that the discharge of water and air are completed before the first peak is measured. The second peak is the result of subsequent surge of steam.

Fig. 3 shows the history of wall pressure. The initial spikes at point A are due to water jet. Air discharge is completed at point B and a bubble, group of large bubbles is formed. It initially expands due to the initial momentum of water given by the air discharge to the pressure lower than ambient pressure as evidenced by the measured wall pressure. Then the bubble pressure reaches to its first minimum at point C, where the bubble size is the maximum. The subsequent oscillation of the bubble explains the rest of the pressure history. It is noteworthy that the negative pressure peak is larger than the positive peak. This strange phenomenon will be discussed later in this paper.

3. ANALYSIS OF BUBBLE OSCILLATION

Since the examination of the experiment shows that the air discharged through many sparger holes quickly merges into one or several large bubbles, it may be a reasonable assumption to treat the discharged air as a spherical bubble. Although shape of the bubble is not perfect spherical and surface shows undulation, it may be reasonable to treat the bubble as one spherical bubble since the bubble will instantaneously feel the pressure exerted by fluid and the pressure in the bubble is technically homogeneous.

3.1 Rayleigh-Plesset equation

The equation traditionally used for analysis of the bubble oscillation in infinite medium is given by (Brennen, 1995)

$$\frac{p_b - p_\infty}{\rho_L} = R\frac{d^2R}{dt^2} + \frac{3}{2}\left(\frac{dR}{dt}\right)^2 + \frac{4\nu}{R}\frac{dR}{dt} + \frac{2S}{\rho_L R} \qquad (1)$$

where R is the bubble radius, ν is the kinematic viscosity, S is the surface tension coefficient, ρ_L is the water density, p_b is the bubble pressure and the p_∞ is the ambient pressure (atmospheric pressure plus hydrostatic pressure. Based perturbation with small amplitude, the natural frequency of equation is

$$f = \frac{1}{2\pi R_0}\left[\frac{3k(p_\infty - p_v)}{\rho_L} - \frac{2(3k-1)S}{\rho_L R_0} - \frac{8\nu_L^2}{R_0^2}\right]^{1/2} \qquad (2)$$

where k is the polytropic expansion constant.

3.2 Modified Rayleigh-Plesset equation

When the size of the tank is comparable to the size of the bubble, the dynamics of a bubble in a confined medium can be simulated more accurately by introducing the images (source or sink according to the geometrical positions) as shown in Fig 6. The equation of multiple bubble oscillation is given by Utamura(1983):

$$\left(\frac{1}{R_i} - \frac{1}{r_e} + \sum_{j\neq i}^{N}\frac{\sigma}{r_{ij}}\right)\dot{X}_i = \frac{X_i^2}{2R_i^4} - \frac{4\nu}{R_i}\frac{dR_i}{dt} - \frac{2S}{\rho_L R_i} + \frac{\Delta p_{bi}}{\rho_L} \qquad (3)$$

where $X = R^2\dot{R}$ and $\Delta p_{bi} = p_{bi} - p_\infty$ and r_e is the domain of integration around bubble, which is the tank radius in this study. The dot means time derivative. σ is 1 for source and -1 for sink. This equation gives solution for the i_{th} bubble oscillation in the presence of N bubbles including i_{th} bubble, all of which oscillate in phase (for sink out of phase).

For the integration of Equation (1) and (3) the initial conditions of bubble radius, bubble surface velocity, and bubble pressure are 0.675 m, 2.0 m/s, and static pressure at the bubble location. The initial condition is given by

$$\frac{dR}{dt} = \frac{\alpha\dot{m}}{4\pi R^2\rho} \qquad (4)$$

where α is a multiplication factor representing the reduction of bubble surface velocity due to the disintegration of bubble. The initial bubble surface velocity calculated from Equation (4) without considering α is 2.7 m/s, when pressure inside sparger during air discharge is 9 bar. Here α is set as 0.75 considering various loss during the discharge.

3.3 Damping

The kinematic viscosity in the legend of Fig. 6 is unexpectedly larger by several orders of magnitude than usual value. Without such a large value the oscillation blows up during numerical integration. The viscosity plays a role of damping for only very small bubble with a radius of less than 0.01 mm (Leighton, 1994). When the size of a bubble is comparable to the tank the flow pattern of ambient medium is no longer radial, but undergoes tortuous stream path and the flow will be highly turbulent. In this circumstance the theory, which results in the equation (1) seems no longer valid. The equation (1) is derived based on Euler equation and force balance at the lamina of bubble surface, where only principal

stress, σ_{rr}, is considered and neglecting, non-principal stresses, $\sigma_{r\theta}$ and σ_{rz}, which obviously are no more negligible when the tank size is comparable to the bubble size. The kinematic viscosity, ν, should incorporate the eddy viscosity due to turbulence. For the solution of bubble oscillation with the consideration of all of the abovementioned argument, the idea of empirical constant may be adopted as having been done in hydraulics, such as pressure drop coefficient. Thus kinematic viscosity is replaced with appropriate value of pressure drop coefficient, which is 1.5 for this study, which is several orders of magnitude large than laminar viscosity.

The pressure history obtained by integrating equation (3) with increased viscosity is compared with the test result in Fig. 5. The pressure peak and the frequency are well reproduced by the calculation.

4. RESULTS AND DISCUSSION

As shown in Fig. 5, the frequency of oscillation increases slightly as the oscillation continues. The dominant (lowest) frequency calculated from the time interval between points D and E is 3.2 Hz, whereas the frequency obtained from integration of Equation (1) and simple calculation by Equation (2) is 5.65 Hz and 5.60 Hz, respectively, where p_∞ is atmospheric pressure plus hydrostatic head of submergence, 2.7 m. The frequency obtained by integrating Equation (3) with the same condition as those of the experiment is 2.79 Hz. The deviation from the experimental result, 3.2 Hz can be attributed to the fact that the actual bubble cloud may not be of a perfect spherical shape and group of large bubbles including small. It is known that the oscillation frequency of bubble cloud is higher than that of a single bubble when the total gas volumes of bubble cloud is the same as that of single bubble (Brennen, 1995). It seems that the Equation (3) reproduces the oscillation of an air bubble in a tank reasonably well. The discharge pressure does not give significant effect on the oscillation and the pressure peak.

4.1 Influence of image layers

The image of a source across the free surface is a sink and that across the wall is a source. The image layers should be constructed like a diamond shape as shown in Fig. 6, otherwise, the converged solution cannot be obtained. When there is no free surface all the images of a source are sources, and in this case the third term in the bracket of left hand side of Equation (2), where σ is 1, goes to infinity resulting in no oscillation. When there is one free surface as is in this study, the situation becomes quite different. The term, where σ is 1 or -1 depending on the type of image, asymptotically converges to some. In Fig. 7 the effect of image layers are shown. For only one layer the third term in the bracket of Equation (3) is 1.7, while the converged value for 100 layers is 3.89. The oscillation frequency shows also a significant change, from 3.48 to 2.68 Hz, Therefore, unless the number of layers is sufficiently large we may end up with an erroneous answer. Especially when the number of layers less than 10 gives a completely wrong answer. The peak pressure shows the same trend.

4.2 Influence of tank size

The base dimensions are linearly increased by multiplying the magnification factor in order to instigate the effect of tank size on the bubble oscillation. The magnification factor is not applied to vertical dimension, since what we want to see is the effect of horizontal dimension. Fig. 8 shows the effect of tank size on the frequency, peak pressure, and potential, $\sum_{j\neq i}^{N} \frac{\sigma}{r_{ij}}$. The potential is asymptotically converged to 0.31 and the frequency also converges in similar manner to 4.65 Hz, while peak pressure decreases as frequency decreases from 52 kPa to 32 kPa. The result is quite different from the Utamura's(1983) results such that the frequency and peak pressure decrease as distance between bubble decreases or tank radius increases. The difference may come from the fact that he studied the effect of distance between bubbles in infinite medium rather than in confined tank. The frequency converges to the certain value as tank size increases, however its value is 4.65 Hz for tank radius of 50 times the base dimension, which is lower than 5.66 Hz or 5.75 Hz. It seems that the effect of images is still felt by the original bubble, despite of considerable tank size and long distance between bubbles. The bubble oscillating in a confined tank will never be the same as free oscillation in infinite medium. It may be the result of assumption of incompressibility. When the domain is very much larger than the bubble size small compressibility may come into play and the bubble will eventually oscillate freely as if it is in infinite medium.

5. ACKNOWLEDGMENTS

This research has been performed as a part of the long-term nuclear energy development program supported by Ministry of Science and Technology of Korea.

REFERENCES

Bae, Y. Y., Kim, H. Y., Park, J. K. "Analysis of flow transients in a pipe with sparger and load reduction ring," Int'l Communications in Heat and Mass Transfer, Vol. 27 (8), pp. 1131-1142, 2000.

Brennen, C. E., *Cavitation and Bubble Dynamics*, Oxford University Press, 1995.

Leighton, T. G., *The Acoustic Bubble*, Academic Press, p 188, 1994.

Rayleigh, Lord, "On the pressure developed in a liquid during the collapse of a spherical cavity," Phil. Mag., Vol. 34, pp. 94-98, 1917.

Su, T. M., "Safety/Relief Valve Quencher Loads: Evaluation for BWR Mark II and III Containment," NUREG-0802, USNRC, 1982.

Utamura, Motoaki "An analysis of multiple bubble behavior in a BWR suppression pool," 2nd Int'l Topical Meeting on Nuclear Thermal hydraulics, ANS Santa Barbara, CA Jan 11-13, 1983.

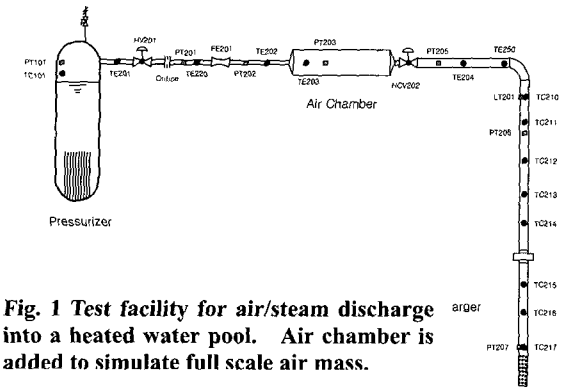

Fig. 1 Test facility for air/steam discharge into a heated water pool. Air chamber is added to simulate full scale air mass.

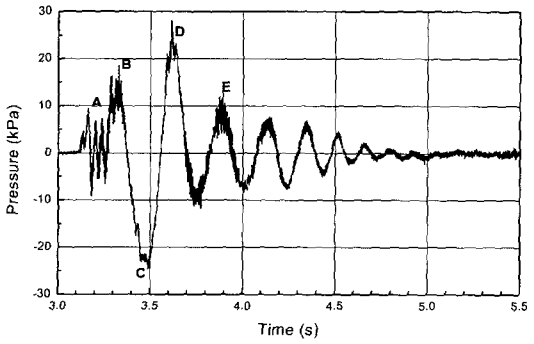

Fig. 2 Typical wall pressure history (CPT-3).

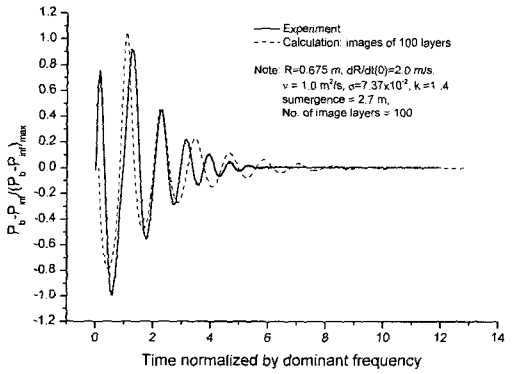

Fig. 5 Comparison of experimental result with numerical simulation by integration of Eq. (1).

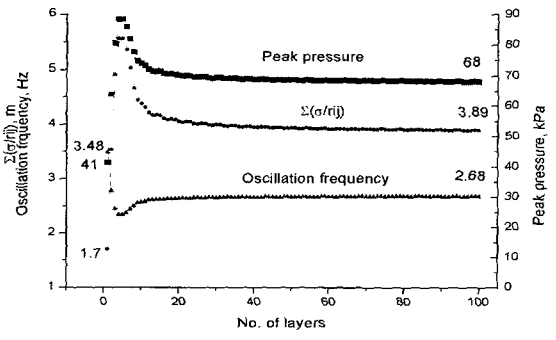

Fig. 7 Effect of number of image layers on the potential of images and oscillation frequency.

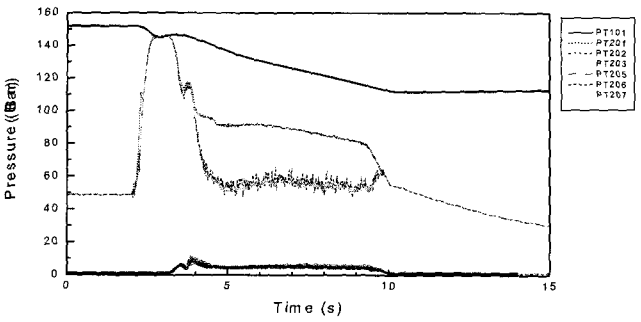

Fig. 3 Pressure variation at the various locations during blowdown.

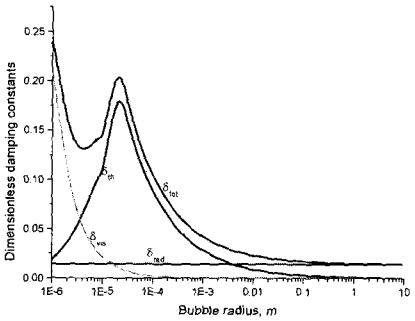

Fig. 4 Dimensionless damping coefficient (viscous, thermal, radiation) versus bubble radius.

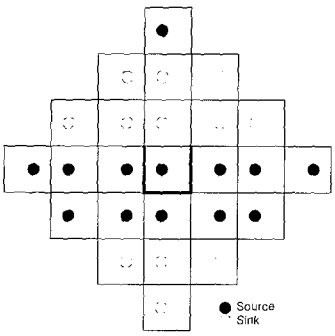

Fig. 6 Distribution of sources and sinks. In front and rear direction sources and

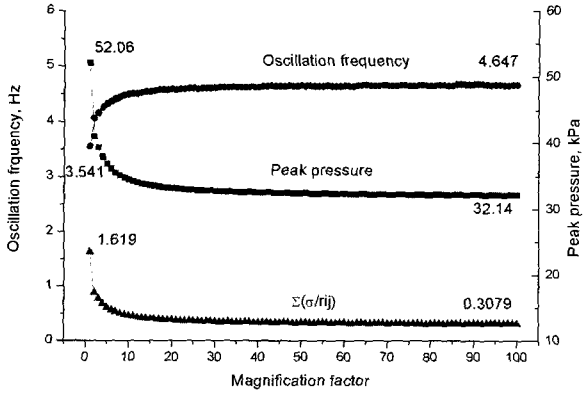

Fig. 8 Effect of tank size on the potential of images and oscillation frequency. Linear dimension of tank is multiplied by magnification factor